Eur. Phys. J. A (2023) 59:52
https://doi.org/10.1140/epja/s10050-023-00956-2

THE EUROPEAN PHYSICAL JOURNAL A

Review

Recent nucleosynthesis in the solar neighbourhood, detected with live radionuclides

Gunther Korschinek[a], **Thomas Faestermann**

Technical University of Munich, Physics Department, James-Franck-Str. 1, D85748 Garching, Germany

Received: 20 October 2022 / Accepted: 17 February 2023 / Published online: 21 March 2023

Communicated by Nicolas Alamanos

Abstract In this article we try to summarize all information, gathered in the last three decades, on short-lived (order of Myr) radionuclides found in the Solar System with interstellar origin, most probably due to stellar processes like supernovae. The most important isotope is ^{60}Fe, but we discuss also information on ^{26}Al, ^{244}Pu and ^{53}Mn. We describe the environment of the Solar System during the past $\approx$ 10 Myr as well as the likely locations where the supernovae occured. Confirming evidence has been found in the composition and energy distribution of galactic cosmic rays. Finally, we discuss the effects that the recent supernova activity might have had on Earth's climate and biosphere.

1 Introduction

Practically all atomic nuclei heavier than oxygen, found in the Solar System (SS), have been formed in earlier stellar processes, i.e. more than 4.5 Gyr ago. The fact that stellar nucleosynthesis still occurs in our Galaxy has been proven by the observation of γ-radiation from radioactive nuclei, like ^{26}Al, ^{60}Fe, or ^{44}Ti (e.g. [1,2]). Since Earth's atmosphere is not transparent for γ-rays, these observations have been made by instruments on satellites like INTEGRAL. The time scale here is given by the half-lives of the radionuclides, not longer than a few Myr. In 1996, the first sentence of this paragraph was somehow questionned. In two publications [3,4] the idea was brought forward, to search on Earth for live (not yet decayed) radioactivities which were produced in core collapse supernovae (SNe) rather close to the SS and entered Earth. Ellis et al. [3] suggested to search for the nuclides with half-lives in the Myr region ^{10}Be, ^{26}Al, ^{36}Cl, ^{53}Mn, ^{60}Fe, ^{129}I, ^{146}Sm, and ^{244}Pu. They discussed also the background due to cosmic ray production of these nuclides in extraterrestrial material and of fission of actinide nuclei. The suggestion from Munich [4] only discussed ^{60}Fe because for lighter nuclides and those with $80 \leq A \leq 150$ the backgrounds from cosmic rays and fission appeared to be dominant, whereas ^{60}Fe cannot be strongly produced with proton induced reactions on the dominant extraterrestrial target elements (ranging up to Ni). There also the detection method is clearly proposed, namely instead of the detection of the decay radiation the direct determination of the nuclide by nuclear charge and mass with the method of accelerator mass spectrometry (AMS). The Munich AMS setup with a gas filled magnet "GAMS"[5] allowed to search for SN formed ^{60}Fe in Earths' deposits for the first time.

Here we want to review the ample experimental information which has been obtained since then, mainly by the labs in Munich, Vienna, Canberra and Sydney. In addition to ^{60}Fe, also ^{244}Pu and ^{53}Mn of extra-solar origin have been detected. We describe also the environment of the Sun in the past millions of years and possible consequences of the recent SN activity on Earth.

2 Detection method: accelerator mass spectrometry (AMS)

AMS is the only method to determine the ultra-low ratios of ^{60}Fe/Fe and ^{53}Mn/Mn of SN material as deposited, and found on Earth and on the Moon [6–11]. In case of the long-living radioisotopes ^{60}Fe and ^{53}Mn solely two AMS setups at tandem accelerators were able to achieve the required sensitivities, the one situated near Munich (jointly operated by both major Munich universities LMU and TUM - meanwhile shut down) and the other at the Australian National University (ANU) in Canberra. Both were able to deliver high enough energy in conjunction with dedicated detection systems, as needed to suppress any possible background events. Details of the Munich and ANU (Canberra) system can be found in

[a] e-mail: korschin@tum.de (corresponding author)

reference [5] and references [12,13], respectively. For ^{244}Pu the labs in Vienna (VERA) [14] and Sydney (ANSTO) [15] with their small accelerators could compete and efficiently determine concentrations, because for ^{244}Pu the determination of the mass number is sufficient for identification, since ^{244}Pu is the only long lived iosobar. Thus ^{244}Pu can be detected as well by other AMS laboratories which are able to magnetically transport these high-rigidity particles and are equipped with appropriate detector systems.

3 Detection of radionuclides

3.1 Radionuclides on Earth

3.1.1 ^{60}Fe

One of the most promising isotopes to search for SN produced radioactivity on Earth is ^{60}Fe. It is predicted to be produced in significant amounts by SNe [16,17] and the natural abundance on Earth is far below any SN induced signal. There are other long-lived isotopes nearly free of terrestrial background (e.g. ^{146}Sm, ^{182}Hf, ^{244}Pu, ^{247}Cm), however they are formed in SNe in much smaller quantities. In addition ^{60}Fe has a half-life of 2.61 ± 0.04 Myr [18,19], long enough to survive transport to Earth. It is believed that ^{60}Fe and other radioisotopes are delivered to Earth in form of dust of grain size larger than 0.3 μm; radiation pressure prevents smaller interstellar dust grains to reach the innermost part of the solar system [20]. There are only few deposits which are suitable to reveal a clear signal for long time-periods in Earth's history like hydrogenetic ferromanganese crusts [21] with growth rates of only a few mm/Myr. The analysis of dated depth layers can reveal an isotopic anomaly of ^{60}Fe/Fe. A first measurement [6] in a deep ocean ferromanganese crust showed an excess of ^{60}Fe. A highly significant increase of ^{60}Fe, 2.8 Myr ago, has been observed in a temporally resolved ferromanganese crust in a follow up study [7]. Figure 1 shows the measured ^{60}Fe/Fe ratios versus the age of the layers without any background or decay correction. It depicts a clear enhancement of the ^{60}Fe/Fe ratio around 2.8 Myr ago indicating a deposit of ^{60}Fe at that time. In Fig. 1 the error bars directly reflect the total number of identfied ^{60}Fe events for a sample. E.g. for the most significant point at 2.8 Myr a total of 43 events of ^{60}Fe was identified.

Similarly as in the mangenese crust, ^{60}Fe should show up as well in deep ocean sediments. A first measurement in a marine sediment showed a broad distribution covering the range from about 2 to 3 Myr. [22]. The results did not reveal a signal as expected with the traversal of the SS by a young SN shock wave. The broad distribution points however to an interaction of the SS with a SN ejecta that has considerably slowed down. To achieve a better resolved signal in a deep ocean sediment, measurements in fractions of two independent Pacific Ocean sediment cores have been performed. The fractions were magnetofossils, the fossilized chains of magnetite crystals produced by magnetotactic bacteria. The selectively extracted Fe from magnetofossils was expected to be minimized by any dilution from large-grained mineral phases. The results show that the ^{60}Fe signal onset occurs around 2.6 Myr to 2.8 Myr, and terminates around 1.7 Myr ago, and peaks at about 2.2 Myr [9].

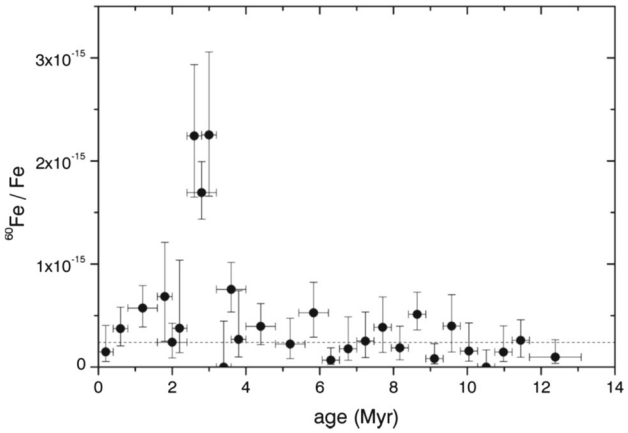

Fig. 1 ^{60}Fe/Fe ratios versus the age of the layer. The data are not corrected for radioactive decay, background, and uptake of iron into the crust. The vertical error bars correspond to a confidence level of 68.3%; the horizontal error bars indicate the time interval covered by the layer. The background level of 2–4 $\times 10^{-16}$ is indicated by the dashed line. Figure and caption adopted from [7]

Confirming and extended studies [8] have been done on deep-sea archives, two Pacific FeMn crust samples, two Atlantic FeMn nodules, and four sediment cores (Eltanin). Their results, Fig. 2, show ^{60}Fe interstellar influxes onto Earth at 1.5–3.2 Myr ago. In addition to previous measurements, they claim another weak signal between 6.5–8.7 Myr ago in FeMn Crust-1.

Work by Basu et al. [23] questioned the SN origin of the ^{60}Fe increase in [7]. They measured the ^{3}He/^{4}He ratio in samples from the same crust and found a strong increase in the ratio 4–5 Myr ago and interpreted this increase to an enhanced deposition of micrometeorites which had been exposed to the flux of galactic cosmic rays (GCR). They argued that the ^{60}Fe increase, as well as the ^{3}He increase, was due to GCR induced reactions on the Ni content of these micrometeorites. In Ref. [22] we argued against this hypothesis because this would require a higher Ni/Fe ratio in the crust than measured. Very recently, Graham and Konrad [24] measured the ^{3}He/^{4}He ratio in samples from the same Eltanin sediment cores as were analyzed for ^{60}Fe by Wallner et al. [8]. They find no correlation between the ^{3}He and ^{60}Fe content and conclude that this supports the hypothesis of a SN origin of the ^{60}Fe.

A summary of locations where enhanced ^{60}Fe/Fe ratios have been measured on Earth is depicted in Fig. 3. All sam-

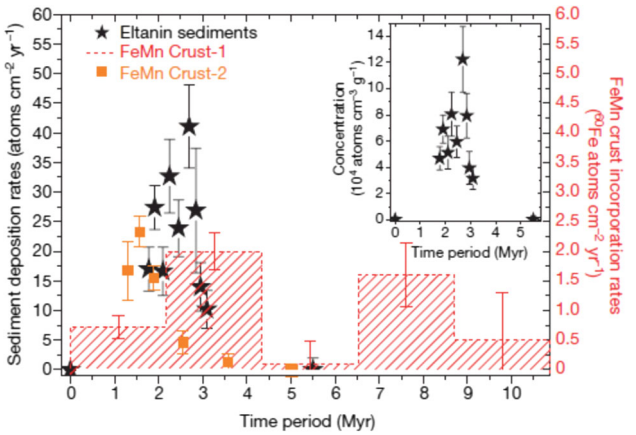

Fig. 2 Deposition rates for sediment (150-kyr averaged data) and incorporation rates for two crust samples. ^{60}Fe concentrations (^{60}Fe per gram) for the sediment are given in the inset; they were on average 6.7×10^4 atoms per gram between 1.7 Myr and 3.2 Myr, but 260×10^4 atoms per gram of crust and 95×10^4 atoms per gram of nodule, reflecting the difference in growth rate and incorporation efficiency. The error bars (1σ Poisson statistics) include all uncertainties and scale with decay correction, so that uncertainties and upper limits become larger for older samples. The absolute ages for the sediment samples have an uncertainty of 0.1 Myr, except for the 5.5-Myr-old sediments, which have an uncertainty of about1 Myr. The age of Crust-1 has an uncertainty of 0.3 Myr and the age of Crust-2 has an uncertainty of 0.5 Myr. Figure and caption are adopted from [8]

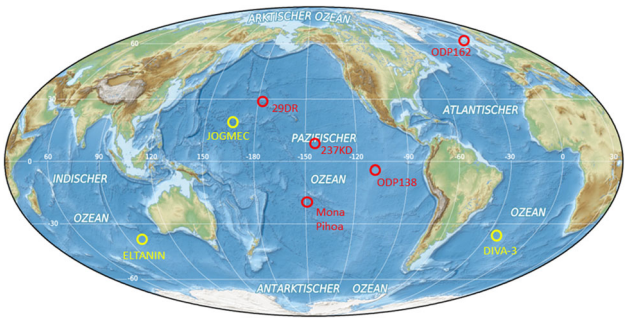

Fig. 3 The different locations where enhanced ^{60}Fe/Fe ratios have been measured either in deep ocean ferromanganese crusts or in sediments. From the locations marked in red (yellow) samples have been analyzed in Munich (Canberra). (The map, in German, with the Pacific in the center is from https://de.wikipedia.org/wiki/Ozean)

ples distributed over the Earth show an ^{60}Fe/Fe anomaly and prove that the signal is spread all over the Earth.

3.1.2 ^{26}Al

Searches for different long-living radioisotopes of SN origin are hampered strongly either by their cosmogenic background or from very low abundance. Thus a study to search for ^{26}Al ($T_{1/2} = 0.717 \pm 0.024$ Myr [25]) in deep-sea sediments where ^{60}Fe has been previously detected, could not find an excess over the cosmogenic background [26]. With the assumption, that there was no alteration of the ^{60}Fe/^{26}Al ratio during the journey until the final deposition on Earth, a lower limit of $0.18^{+0.15}_{-0.08}$ for the local interstellar ^{60}Fe/^{26}Al isotope ratio has been stated. It compares with ratios from nucleosynthesis models which are within the range of $0.05 \leq {}^{60}\text{Fe}/{}^{26}\text{Al} \leq 0.15$.

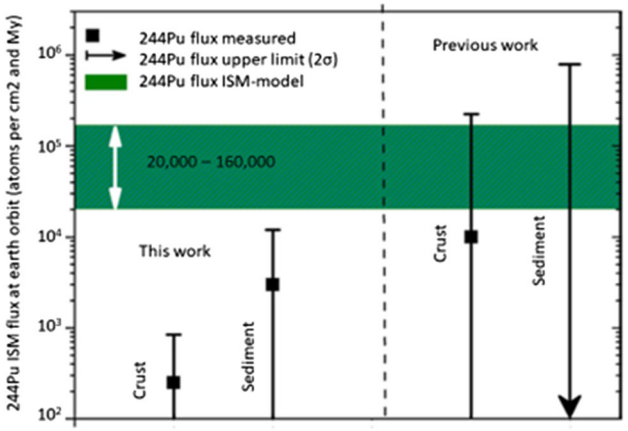

Fig. 4 Figure adopted from [34], it depicts the different measurements in deep-sea crusts and sediments. It compares also with galactic chemical evolution models (shown as green area). Details in Ref. [34]

3.1.3 ^{244}Pu

An important question in nucleosynthesis concerns the site of actinide production. Besides other scenarios a candidate source for the r-process have been core-collapse SNe [27]. To find actinides in correlated (or uncorrelated) layers where ^{60}Fe has been found could support (or challenge) this hypothesis. Best suited in this case is ^{244}Pu as it has a long half-life of 81.3 ± 0.3 Myr [28] and interference of primordial ^{244}Pu is not expected. Previously reported detection [29] of primordial ^{244}Pu on Earth has not been confirmed [30]. First measurements in deep sea manganese encrustations and of pre-bomb depth showed already that the ^{244}Pu signal is weak, but still consistent with a SN signal suggested by the ^{60}Fe data [31,32]. An upper limit of ^{244}Pu in a 1-kg deep-sea dry sediment has been reported by Paul et al. [33]. An elaborated study [34] showed for the first time a clear detection of live interstellar ^{244}Pu in Earth's deep-sea floor combined over the last 25 Myr. The abundances were lower than expected from continuous production in the Galaxy by about 2 orders of magnitude. This large discrepancy could point to a rarity of actinide r-process nucleosynthesis sites. Possible sources could be neutron-star mergers with a small subset of actinide-producing SNe [34].

Figure 4 depicts the different measurements in deep-sea crusts and sediments. It compares also with galactic chemical evolution models (shown as green area). Details in reference [34].

In a follow-up study [35] ^{60}Fe and ^{244}Pu concentrations in further deposits have been determined. While ^{60}Fe is mainly produced in massive stars and ejected in SN explosions, ^{244}Pu is produced in r-process events only. Importantly, the measured ^{244}Pu influx was lower than expected if SNe dominate r-process nucleosynthesis. It has been concluded, that the data were compatible with the Local Bubble (see chapter 4) being a local disturbance of a large-scale Galactic steady-state (from SN enrichment of the ISM occurring more frequently than the radioactive half-life), with less-frequent injections from rarer r-process sources that nevertheless dominate the production of r-process elements, such as neutron-star mergers. The data are also consistent with the hypothesis of a nearby rare event before the time of SS formation that supplied the majority of the SS known inventory of the primordial actinides [35,36]. Also from observations the evidence became compelling during the last decade that the r-process occurs in kilo-novae [37] which are the result of neutron star mergers [38].

3.1.4 ^{53}Mn

Several indications support the SN origin of the ^{60}Fe [39,40]. However, there is also the possibility of ^{60}Fe being formed in asymptotic giant branch (AGB) stars [41–43] (for a recent review on cosmic nucleosynthesis we also refer to Diehl et al. [44]). Despite of a lower nucleosynthesis yield, they could be the origin of the observed ^{60}Fe, as well. Therefore, a solely SN formed radionuclide, such as ^{53}Mn ($T_{1/2} = 3.7 \pm 0.4$ Myr) [45], detected in the same samples as the ^{60}Fe, would be a compelling support for the SN origin of this ^{60}Fe. Until now, ^{53}Mn, formed by nucleosynthesis, has not been detected in the interstellar space because ^{53}Mn decays by electron capture directly to the ground state of ^{53}Cr, hence only low-energy X-rays are emitted, not detectable by space borne detectors. Different to ^{60}Fe, the dominant fraction of the ^{53}Mn in the SS is produced by cosmic rays in dust that originates from asteroid collisions or comets. Compared to interplanetary ^{53}Mn influx on Earth the ^{53}Mn influx via interstellar dust [46] represents only a very small contribution. To evaluate this very small contribution four different crusts, all of them of hydrogenetic origin, and from different locations in the Pacific Ocean have been analyzed for their ^{53}Mn content [11]. All ^{53}Mn/Mn ratios have been calculated at the time of incorporation by means of their age (i.e., corrected for radioactive decay). In a second step the data from the four crusts have been merged as shown in Fig. 5.

For the time period from 1.5 to 4 Myr before present an ^{53}Mn excess concentration in terms of ^{53}Mn/Mn over that expected for cosmogenic production has been found. It confirms the SN origin of the ^{60}Fe. It is also for the first time that SN formed ^{53}Mn has been detected and it is the second positively identified radioisotope from the same SN. Also, the

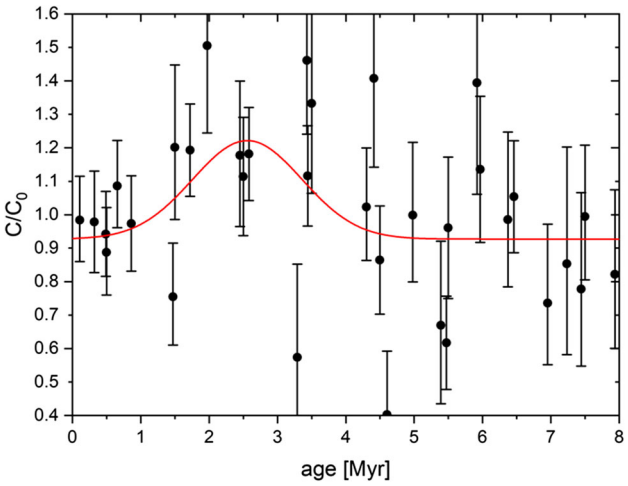

Fig. 5 Merged ^{53}Mn/Mn ratios (C/C_0) from the different crusts at the time of incorporation. The values are normalized to the present ratio C_0. The red curve is the result of a fit of a Gaussian with fixed width $\sigma = 0.8$ Myr. The fitted height is about three times its uncertainty

^{53}Mn/^{60}Fe ratio of about 14 is consistent with that expected for a SN with a 11–25 $M_\odot$ progenitor mass and solar metallicity.

3.2 Interstellar ^{60}Fe on the surface of the Moon

The remnant of a SN which passed the SS and has been detected on Earth [6–9] should leave a signature, as well, on the solar planetary system and also on Earths' Moon. Hence the detection of a ^{60}Fe signal on another SS body than Earth was of crucial importance to confirm the SN origin. There are significant differences, however, between a signal on the Moon and those on Earth. The ^{60}Fe deposition on Earth until it finally ends in ocean sediments or ferromanganese crusts at different locations is a rather complex process, involving atmospheric and ocean current processes as well as ocean chemistry, to mention only a few. This is rather different for lunar samples. We can assume that the dominant part of the interstellar dust is of larger size $\geq 0.2\,\mu$m [47]. This compares well to lunar dust which comprises also similar size particles. In addition, the impact velocity of interstellar particles can vary over the year as the orbital velocity of the Earth is around 29 km/s which have to be considered with respect to the initial velocity of the particles, depending on the direction of the impact. There are several estimations on the trapping of dust particles on the Moon [48,49]. We should point out however that any experimental data input is based on a detector where the impact of dust particles happened on a solid target. This is diverse at the dust layer on the Moon which is of different composition and morphology. The dust projectiles tend to interact with individual grains and not with bulk regolith. Hence the impact of dust particles with lunar

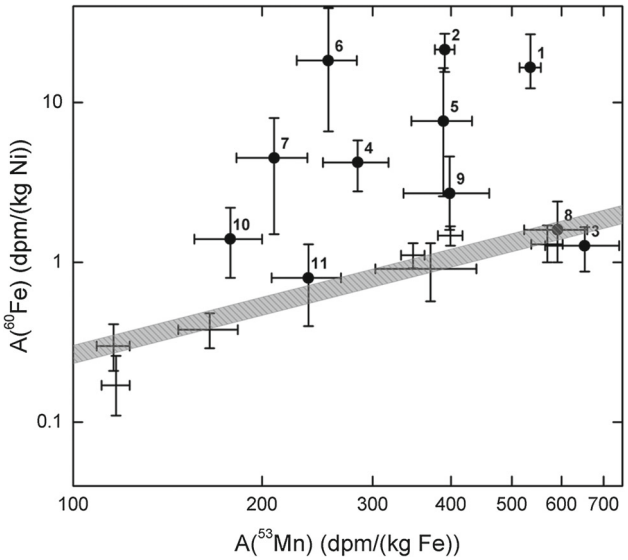

Fig. 6 Measured activities of ^{60}Fe versus ^{53}Mn in meteoritic and lunar samples. Units are disintegrations per minute per kilogram of Fe and Ni, for ^{53}Mn and ^{60}Fe, respectively. Samples 1 through 11 (filled points) are lunar samples; the other values (error bars only) are for iron meteorites. The labeling of the data points is specified in Table I in [10]. The shaded bar indicates the error band for cosmogenically produced ^{53}Mn and ^{60}Fe activities in meteorites. The error bars indicate the 1σ confidence level [50]. Figure and captions adopted from [10]

dust is rather complex, and unfortunately no experimental data are available. This hampers theoretical estimations.

Thus, experimental information and a confirmation of the SN origin of ^{60}Fe in measurements of lunar samples are of essential importance. Therefore, ^{60}Fe and ^{53}Mn ratios from selected samples from different Apollo missions [10] have been determined. Besides of SN origin, ^{60}Fe is also formed in nuclear reactions by solar and galactic cosmic rays (GCR) with the heavy Ni isotopes in lunar soil. This adds to interstellar ^{60}Fe. ^{53}Mn is formed dominantly by GCRs through the (p,α) reaction on ^{56}Fe whereas the interstellar contribution is negligible. Figure 6 shows the measured activities of lunar and meteoritic samples. The lunar samples are labeled by number from 1 to 11. The data points (3, 8, 11) have a complicated history, as described in [10], they have activities comparable to the meteorite samples along the shaded area. All others show an enhanced ^{60}Fe activity relative to the Ni content (dpm/kg Ni). The meteoritic radionuclides are cosmogenically produced. In both cases the radionuclides ^{60}Fe and ^{53}Mn are formed by nuclear reactions of cosmic rays with Ni and Fe respectively. The shaded bar indicates the error band for the cosmogenically produced ^{53}Mn and ^{60}Fe activities in meteorites. The variation in the meteorite samples is because of the differences in the preatmospheric sizes of the precursor meteoroids and the depths of the samples.

As the surface of the Moon is constantly mixed and stirred by the impact of micrometeorites and larger objects [51], a process called "gardening", the deposited radionuclides are distributed in a layer of a few mm thickness a few Myr after deposition. The origin of the lunar samples was of different depth which is reflected in the scatter of the data of the lunar samples. Considering the downward distribution of the ^{60}Fe signal due to gardening a decay corrected local interstellar fluence of ^{60}Fe at the time of deposition has been estimated between 0.8×10^8 and 4×10^8 atoms/cm^2 [10]. The data are comparable to other measurements in Earths' reservoirs [7–9], and they support the SN origin.

3.3 Radionuclides today

Information on the most recent deposition on Earth of interstellar material has been obtained by Koll et al. [52]. In this work 500 kg of Antarctic snow, not older than 20 yr, were analyzed with respect to the radionuclides ^{60}Fe and ^{53}Mn. The molten snow water was filtered with a pore size of 2–3 μm. In the filtrate amounts of 5×10^4 atoms ^{60}Fe and 3×10^6 atoms ^{53}Mn were found by AMS. The ^{53}Mn content served, as in the lunar samples (Chapter 3.2), as reference to the cosmic ray produced radioactivities. For the atomic ratio in meteorites ^{60}Fe/^{53}Mn= 0.0019(2)$\times$ [Ni]/[Fe] was used, based on Fimiani et al. [10]. The measured ratio in the filtrate ^{60}Fe/^{53}Mn= 0.017 with an assumed chondritic element concentration [Ni]/[Fe] = 0.055 is about two orders of magnitude higher and proof of a present day interstellar ^{60}Fe input on Earth of about 1.2 atoms $/cm^2/$year. The data base of ^{60}Fe/^{53}Mn ratios in iron meteorites has recently been improved by Leya et al. [53]. The resulting ratio ^{60}Fe/^{53}Mn= 0.00177(7)$\times$ [Ni]/[Fe] is very close to that used earlier [52].

Wallner et al. [54] have also searched for ^{60}Fe in young—compared to the strong input 2–3 Myr ago—sediment cores from the Indian Ocean. The layers covered ages between 1 and 33 kyr and yield ^{60}Fe deposition rates of about 3.5 atoms/cm^2/year. Within the large error bars the five data points are consistent, about three times the present deposition rate in Antarctica [52] and an order of magnitude smaller than the maximum deposition in sediments 2–3 Myr ago [8]. They as well as Koll et al. [55] discuss different scenarios, how the ^{60}Fe could enter the SS. One possibility could be that ^{60}Fe containing dust from earlier SNe resides in the Local Interstellar Cloud (LIC) which the SS entered some 40 kyr ago. To distinguish between the scenarios a determination of the ^{60}Fe content in 50–300 kyr old sediment samples with good time resolution would be important.

4 The surroundings of the Sun during the last millions of years

The Sun is presently inside the Local Bubble (LB), a nearly spherical, almost empty structure surrounded by a shell of dense interstellar medium of atoms, ions, molecules, and dust particles [56,57]. According to Breitschwerdt et al. [39] its origin are explosions of several SNe, starting around 14 Myr ago. The remnants and the swept material from the ambient interstellar medium formed the shell.

Presently, the SS is positioned almost in the center of the LB [58] which has a diameter of about 300 pc. To find the position of the Sun relative to the LB when it passed the remnant of the last SN [39], we can do a crude estimation. With a relative velocity of 15.4 km/s [58] of the SS, and the time of the deposition of the ^{60}Fe on Earth around 2.5 Myr ago [7–9], we estimate the distance to the present position of around 40 pc. These can be compared with Zucker et al. [58] where it is stated that the SS entered the LB around 5 Myr ago. We conclude that the 2.5 Myr event happened inside of the preformed bubble. This seems different in case of the earliest detected ^{60}Fe deposition between around 6.5 Myr until 8.7 Myr ago [8,35]. In this case we find a distance of 120 pc if we consider a mean value of 7.6 Myr. If we compare this with the entrance of the SS into the bubble 5 Myr ago, we see an indication that the ^{60}Fe deposition at about 7.6 Myr should have happened outside of the LB. Origin for this ^{60}Fe signal could be that the SS has collected remnant and swept-up material from the star forming regions indicated as Taurus old and Taurus young [58]. As noted above, a confirmation of the older influx was published in [35] together with a time profile of the 7.6 Myr peak.

There are cloudlets of dense interstellar medium that move inside of the LB. Their origin is discussed in refs. [57,59]. A possible scenario addresses the interaction of the LB with the adjacent loop I bubble [57]. The nearest cloudlets to the SS are the Local Interstellar Cloud (LIC) and the G-Cloud as shown in Fig. 7. The illustration shows the solar neighborhood with the nearby clouds, the LIC and the G-Cloud, and the relative motions, indicated by blue arrows. The SS is located on the margin of the LIC close to the G-Cloud, its' motion is indicated by a yellow arrow. It entered the LIC around 40 kyr ago and will leave it in about 4 kyr [59]. To detect ^{60}Fe deposited from the LIC, as found in deep ocean crusts and sediments [7–9], and even on the Moon [10] could help to establish the origin of the LIC. This question was addressed by Koll et al. [52] by searching for ^{60}Fe in Antarctic snow (see chapter 3.3). The reader is also referred to the later work [54,55].

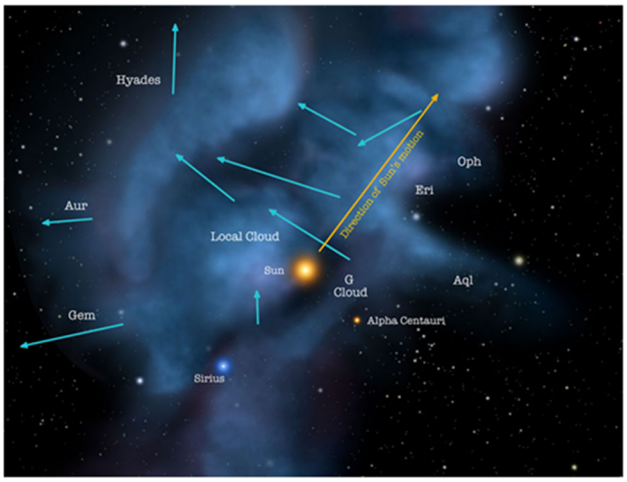

Fig. 7 Solar neighborhood with the nearby Clouds: the LIC and the G-Cloud. The relative motions are indicated by blue arrows. The Solar System is located inside the LIC, its motion is indicated by a yellow arrow. Picture dimensions: 14 pc × 11 pc. Illustration credit: NASA, Goddard, Adler, U. Chicago, Wesleyan

5 Possible locations of the SN activity

Already in 2002, Benitez and colleagues [60] suggested that SN explosions in the Scorpius-Centaurus OB association could be responsible for the ^{60}Fe observed on Earth [6]. Fry, Fields and Ellis [61] discussed the transport of ^{60}Fe, condensed in dust grains, from a SN origin through the interstellar medium, the solar heliosphere and the atmosphere onto Earth (and Moon). They estimate an 8–10 $M_\odot$ SN at a distance around 50 pc as responsible for the ^{60}Fe on Earth. A group around D. Breitschwerdt reacted to the observations of live ^{60}Fe and calculated [39] possible trajectories and masses of possible SN progenitors within a moving group of stars whose surviving members are now in the Scorpius–Centaurus stellar association. They conclude that the closest SN occured 2.3 Myr ago with a progenitor mass of $9.2 M_\odot$, the next closest 1.5 Myr ago with $8.8 M_\odot$, at distances of 91 pc and 96 pc, respectively. Later work by the same group [62,63] discusses also new data and the creation of the LB by earlier SNe (see also chapter 4). Neuhäuser et al. [64] searched in the Scorpius–Centaurus–Lupus group of young stars for runaway stars which had belonged to a binary system, where the heavier partner underwent a SN and only a neutron star remained, not able to bind the partner. They identify from their relative velocities one pair of a runaway star (called ζ Oph) and a radiopulsar which were less than 0.5 pc apart 1.8 Myr ago at a distance of 107 pc from the Sun. The estimated mass of the SN progenitor is 16–18 $M_\odot$. Briceños-Morales and Chanamé [65] studied the SN activity in the OB association Upper Scorpius and attribute this runaway star also to the Lupus I cloud and a SN 1.8 Myr ago.

6 Cosmic rays

SNe not only eject huge amounts of matter ($> 2M_{\odot}$), containing also freshly produced radionuclides in a rapidly expanding shock front, but they also accelerate nuclei, mostly protons, in these shock fronts to relativistic velocities. A number of spacecrafts is equipped with instruments to detect these cosmic ray particles and to measure their energy and even their mass and charge number, thus uniquely identfying the detected nucleus. On board of NASA's Advanced Composition Explorer (ACE), which orbits around the Lagrange point L1, 1.5×10^6 km from the Earth, operates the Cosmic Ray Isotope Spectrometer (CRIS). In 2016 its result for an observation time period of 17 years was published [66]. Indeed, in this paper Binns et al. report on a clean identification of 15 ^{60}Fe nuclei in an energy range between 200 and 500 MeV/nucleon or velocities $0.56 \leq v/c \leq 0.76$. Because the neighbouring isotope ^{59}Fe has a half-life of only 44 d it does not appear in the spectrum and allows for that clean identification. They determined the number ratio relative to the most abundant stable iron isotope as ^{60}Fe/^{56}Fe $= 7.5(2.9) \times 10^{-5}$ at the source. In view of the half-life of ^{60}Fe of 2.6 Myr [18,19] they conclude an upper limit for the time between nucleosynthesis and acceleration of a few Myr. The responsible SNe should have occured < 620 pc from the Sun and they see the Sco-Cen OB association and the Orion OB1 association as the main contributors to the observed ^{60}Fe nuclei. In fact, for the production of these cosmic rays two SNe are required, one for the nucleosynthesis and one for the acceleration, because no ^{59}Ni ($T_{1/2} = 76$ kyr [67]) was observed in the cosmic rays, meaning that it had decayed before acceleration [68].

Just recently, Boschini et al. [69] have analyzed cosmic ray spectra of heavier nuclei including recent data of the Alpha Magnetic Spectrometer (AMS-02) on board of the ISS [70]. They find an excess in the spectrum of stable iron nuclei in the energy range below 2 GeV/nucleon which they ascribe to the same origin as the excess in the isotope ^{60}Fe, namely the past SN activity in the LB.

In addition, already the energy spectra of protons (in the energy range TeV to PeV), positrons (30–300 GeV) and antiprotons (30–300 GeV) differ from those of the average Galactic spectra. According to Kachelrieß et al. [40] these deviations can best be understood if they assume a local cosmic ray source between 2 and 4 Myr old which ejected about 10^{50} erg and happened on a galactic magnetic field line which passed the Sun at a distance not more than 100 pc. The only plausible assumption for this source are SNe.

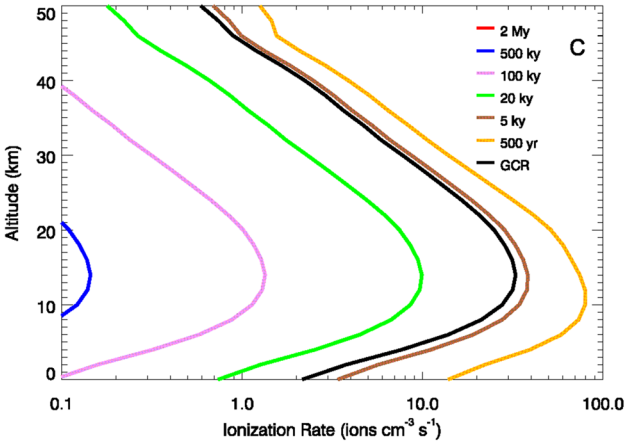

Fig. 8 Additional ionization in the atmosphere for different times after a SN 100 pc from the Sun (from Thomas et al. [74])

7 Effects on the climate and biosphere

One of the first discussions on biological effects of a nearby SN has been done by Terry and Tucker [71]. In a different approach to this problem, following the line of Ruderman [72], who had studied the depletion of the ozone layer, Ellis and Schramm [73] discussed the influence of a close SN on the Earth. For a distance of about 10 pc the direct thermal influence would be negligible. The main effect would be the ozone destruction by γ radiation and cosmic rays. With the shielding ozone layer missing, the solar UV radiation would damage life on Earth and could lead to a mass extinction.

More recently, Melott, Thomas and coworkers [74–77] discuss possible consequences on Earth of SN activity at distances between about 50 and 150 pc with the putative SNe [7,8] between 2 and 10 Myr in mind. In Fig. 8 we show their calculation of the increase of ionization in the atmosphere due to a SN at a distance of 100 pc. They see an effect for life on Earth mainly due to the inrease of radiation, muon irradiation on the ground will increase by a factor of 20. Another effect of the increased atmosperic ionization could be an increase in the frequency of lightning. Lightning plays a strong role for the deposition of nitrate out of the atmosphere. Lightnings are also a cause for wildfires and thus for a conversion of woodland into savanna.

Marsh and Svensmark [78] discuss a different mechanism: the correlation between galactic cosmic radiation and cloud formation below a height of 3.2 km. Ionizing radiation in the atmosphere could help to form aerosol particles that can act as cloud condensation nuclei. The cloud conditions naturally have a significant impact on the global radiation budget. This correlation of cosmic rays and climate is further dicussed by Usoskin and Kovaltsov [79] and also by Kirkby [80] for different geological time scales up to 500 Myr. Kirkby also discusses the CLOUD experiment that has been set up at

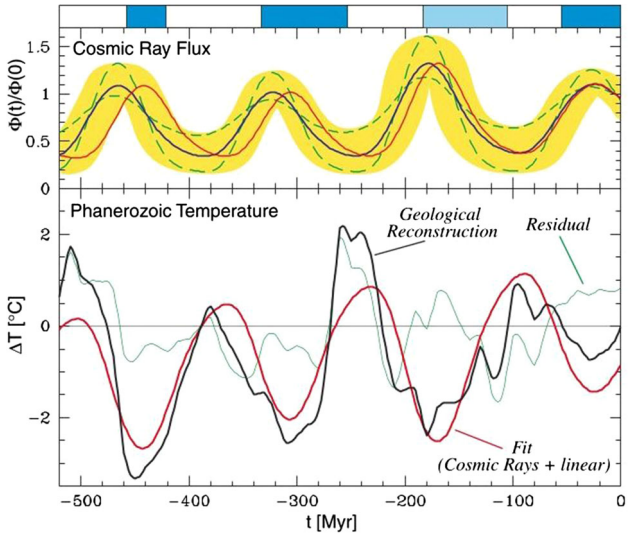

Fig. 9 Correlation of the ocean temperature over the past 500 Myr (lower diagram, reconstructed from ^{18}O in calcite shells) with the change of cosmic radiation flux (upper diagram) when the Sun oscillates through the Galactic plane (from Shaviv and Veizer [81])

CERN which uses protons with energies up to 26 GeV from the proton synchrotron to experimentally study the effect of high-energy protons on the formation of aerosols or on cloud droplets directly. In Fig. 9 he showed us how strongly cosmic ray intensity and global temperature are correlated following an analysis of Shaviv and Veizer [81]). Just recently, Orgueira et al. [82] have tested with a statistical analysis the hypothesis that an increase of cosmic rays due to SN activity, in addition to a lowering of the geomagnetic field intensity, could have led to the global cooling about 2.5 Myr ago, just at the Pliocene-Pleistocene boundary. They find such a scenario quite probable. In a recent preprint [83] Opher and Loeb describe a little different scenario for a change of Earth's climate: When the solar system was passing through a cold cloud (e.g. the Local Leo Cold Cloud) some 2 Myr ago, the heliosphere shrunk to a scale smaller than the Earth's orbit. Therefore Earth was exposed to a neutral hydrogen density of up to 3000 cm^{-3}. This could have had drastic effects on Earth's climate.

When we look at the temperature changes during the past 500 Myr (Fig. 10, taken from δ^{18}O data) and look at the beginning of the Pleistocene (the geologists put it at 2.588 Myr ago), we see the drop in global temperature, i.e. the period of glaciation. It just coincides with the beginning of ^{60}Fe deposition on Earth which we ascribe to SN activity in the neighbourhood of the Sun. These colder temperatures are seen as the cause of the conversion in Africa of wood land into savanna or grassland [84]. Already in our first report on the time resolved input of ^{60}Fe onto Earth [7] and later on [85,86] we speculated on a correlation of SNe with the Pliocene-Pleistocene climate change and possible consequences on the terrestrial fauna.

Another cause for a larger climate change at that time could have been the closing of the Isthmus of Panama which for a long time was dated as 3.5 Myr ago. However, a detailed analysis of molecular and fossil data [87] comes to the conclusion that the closure was completed by 6 Myr ago, i.e. long before the Pliocene-Pleistocene boundary.

Paleoanthropologists agree that this change of climate and habitat in Eastern or Southern Africa is responsible for the evolution of the genus Homo [88,89]. Just about 2.5 Myr ago the Homo Habilis and Homo Rudolfensis appeared [90], the first species that used speech, tools and developed culture. Likewise, in recent work by Timmermann et al. [91], a team of climatologists and paleoanthropologists links the appearance of later species of Homo: Homo heidelbergensis, Homo neanderthalensis and even Homo sapiens to climate changes in Africa and Eurasia and the adaptation of Homo to different climates.

Of course, there is no solid proof, but the idea is appealing that SNe have triggered the climate change at the Pliocene-

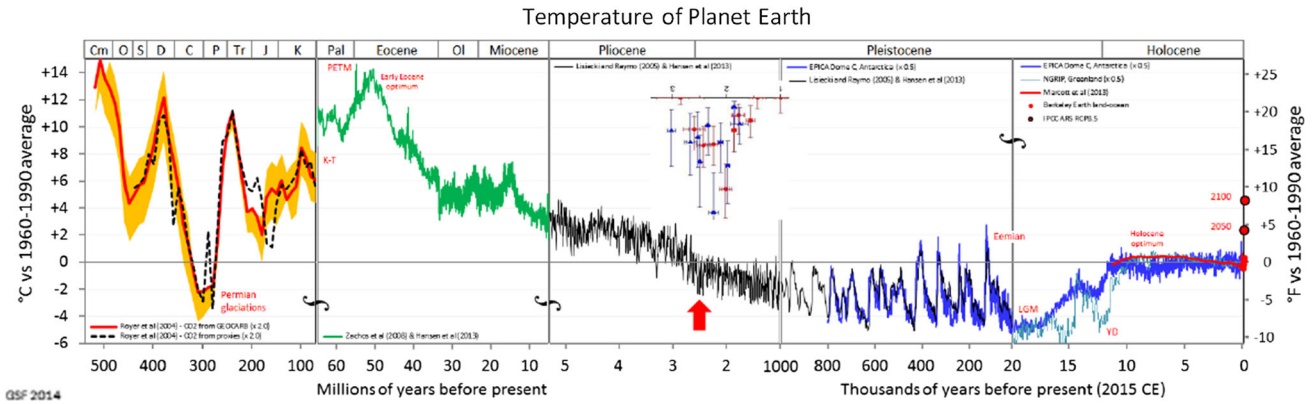

Fig. 10 Global temperature for the past 500 Myr with differing time scales (from Wikipedia Commons, author: Glen Fergus). The arrow marks the beginning of the Pleistocene. Inserted is, on the same time scale (upside-down), a copy of the ^{60}Fe profile of Ludwig et al. [9]

Pleistocene boundary and, thus, the development of the genus Homo.

Funding Information Open Access funding enabled and organized by Projekt DEAL.

Data availibility statement This manuscript has no associated data or the data will not be deposited. [Authors' comment: Since this is a review article, it is not connected to any specific data, the data are all in the referenced publications.]

References

1. N. Prantzos, R. Diehl, Radioactive ^{26}Al in the galaxy: observations versus theory. Phys. Rep. **267**, 1–69 (1996)
2. R. Diehl, Nuclear astrophysics lessons from INTEGRAL. Rep. Prog. Phys. **76**(2), 026301 (2013)
3. J. Ellis, B.D. Fields, D.N. Schramm, Geological Isotope Anomalies as Signatures of Nearby Supernovae. Astrophys. J. **470**, 1227 (1996)
4. G. Korschinek, T. Faestermann, K. Knie, C. Schmidt, ^{60}Fe, a promising AMS isotope for many applications. Radiocarbon **38**(1), 68–69 (1996)
5. K. Knie, T. Faestermann, G. Korschinek, G. Rugel, W. Rühm, C. Wallner, High-sensitivity AMS for heavy nuclides at the Munich Tandem accelerator. Nucl. Inst. Methods Phys. Res. B **172**(1–4), 717–720 (2000)
6. K. Knie, G. Korschinek, T. Faestermann, C. Wallner, J. Scholten, W. Hillebrandt, Indication for supernova produced ^{60}Fe activity on Earth. Phys. Rev. Lett. **83**(1), 18–21 (1999)
7. K. Knie, G. Korschinek, T. Faestermann, E.A. Dorfi, G. Rugel, A. Wallner, ^{60}Fe anomaly in a deep-sea manganese crust and implications for a nearby supernova source. Phys. Rev. Lett. **93**(17), 171103 (2004)
8. A. Wallner, J. Feige, N. Kinoshita, M. Paul, L.K. Fifield, R. Golser, M. Honda, U. Linnemann, H. Matsuzaki, S. Merchel et al., Recent near-Earth supernovae probed by global deposition of interstellar radioactive ^{60}Fe. Nature **532**(7597), 69–72 (2016)
9. P. Ludwig, S. Bishop, R. Egli, V. Chernenko, B. Deneva, T. Faestermann, N. Famulok, L. Fimiani, J.M. Gómez-Guzmán, K. Hain et al., Time-resolved 2-million-year-old supernova activity discovered in Earth's microfossil record. Proc. Natl. Acad. Sci. **113**(33), 9232–9237 (2016)
10. L. Fimiani, D.L. Cook, T. Faestermann, J.M. Gómez-Guzmán, K. Hain, G. Herzog, K. Knie, G. Korschinek, P. Ludwig, J. Park et al., Interstellar ^{60}Fe on the surface of the Moon. Phys. Rev. Lett. **116**(15), 151104 (2016)
11. G. Korschinek, T. Faestermann, M. Poutivtsev, A. Arazi, K. Knie, G. Rugel, A. Wallner, Supernova-produced ^{53}Mn on Earth. Phys. Rev. Lett. **125**(3), 031101 (2020)
12. L.K. Fifield, S.G. Tims, T. Fujioka, W.T. Hoo, S.E. Everett, Accelerator mass spectrometry with the 14UD accelerator at the Australian National University. Nucl. Inst. Methods Phys. Res. B **268**(7–8), 858–862 (2010)
13. A. Wallner, L.K. Fifield, M.B. Froehlich, D. Koll, G. Leckenby, M. Martschini, S. Pavetich, S.G. Tims, D. Schumann, Z. Slavkovská, Accelerator mass spectrometry with ANU's 14 million volt accelerator. Nucl. Inst. Methods Phys. Res. B **534**, 48–53 (2023)
14. W. Kutschera, P. Collon, H. Friedmann, R. Golser, P. Hille, A. Priller, W. Rom, P. Steier, S. Tagesen, A. Wallner, E. Wild, G. Winkler, VERA: a new AMS facility in Vienna. Nucl. Inst. Methods Phys. Res. B **123**(1–4), 47–50 (1997)
15. M.A.C. Hotchkis, D.P. Child, M.B. Froehlich, A. Wallner, K. Wilcken, M. Williams, Actinides AMS on the VEGA accelerator. Nucl. Inst. Methods Phys. Res. B **438**, 70–76 (2019)
16. D.D. Clayton, New prospect for gamma-ray-line astronomy. Nature **234**(5327), 291–292 (1971)
17. S.E. Woosley, T.A. Eaver, The evolution and explosion of massive stars. II. Explosive hydrodynamics and nucleosynthesis. Astrophys. J. Suppl. **101**, 181 (1995)
18. G. Rugel, T. Faestermann, K. Knie, G. Korschinek, M. Poutivtsev, D. Schumann, N. Kivel, I. Günther-Leopold, R. Weinreich, M. Wohlmuther, New measurement of the ^{60}Fe half-life. Phys. Rev. Lett. **103**(7), 072502 (2009)
19. A. Wallner, M. Bichler, K. Buczak, R. Dressler, L.K. Fifield, D. Schumann, J.H. Sterba, S.G. Tims, G. Wallner, W. Kutschera, Settling the Half-Life of ^{60}Fe: fundamental for a versatile astrophysical chronometer. Phys. Rev. Lett. **114**(4), 041101 (2015)
20. N. Altobelli, S. Kempf, H. Krüger, M. Landgraf, M. Roy, E. Grün, Interstellar dust flux measurements by the Galileo dust instrument between the orbits of Venus and Mars. J. Geophys. Res. (Space Physics) **110**(A7), A07102 (2005)
21. A.C. Aplin, D.S. Cronan, Ferromanganese oxide deposits from the Central Pacific Ocean, I Encrustations from the Line Islands Archipelago. Geochim. Cosmochim. Acta **49**(2), 427–436 (1985)
22. C. Fitoussi, G.M. Raisbeck, K. Knie, G. Korschinek, T. Faestermann, S. Goriely, D. Lunney, M. Poutivtsev, G. Rugel, C. Waelbroeck, A. Wallner, Search for supernova-produced ^{60}Fe in a marine sediment. Phys. Rev. Lett. **101**(12), 121101 (2008)
23. S. Basu, F.M. Stuart, C. Schnabel, V. Klemm, Galactic-cosmic-ray-produced ^{3}He in a ferromanganese crust: any supernova ^{60}Fe excess on Earth? Phys. Rev. Lett. **98**(14), 141103 (2007)
24. D.W. Graham, K. Konrad, Supernova versus cosmic ray origin for exotic nuclides in geomaterials: a test using ^{3}He with ^{60}Fe in marine sediments. Geochim. Cosmochim. Acta (2022)
25. M.S. Basunia, A.M. Hurst, Nuclear data sheets for A = 26. Nucl. Data Sheets **134**, 1–148 (2016)
26. J. Feige, A. Wallner, R. Altmeyer, L.K. Fifield, R. Golser, S. Merchel, G. Rugel, P. Steier, S.G. Tims, S.R. Winkler, Limits on supernova-associated ^{60}Fe/^{26}Al nucleosynthesis ratios from accelerator mass spectrometry measurements of deep-sea sediments. Phys. Rev. Lett. **121**(22), 221103 (2018)
27. A. Bartlett, J. Görres, G.J. Mathews, K. Otsuki, M. Wiescher, D. Frekers, A. Mengoni, J. Tostevin, Two-neutron capture reactions and the *r* process. Phys. Rev. C **74**, 015802 (2006)
28. C.D. Nesaraja, Nuclear data sheets for A=244. Nucl. Data Sheets **146**, 387–510 (2017)
29. D.C. Hoffman, F.O. Lawrence, J.L. Mewherter, F.M. Rourke, Detection of plutonium-244 in nature. Nature **234**(5325), 132–134 (1971)
30. J. Lachner, I. Dillmann, T. Faestermann, G. Korschinek, C. Lierse, M. Poutivtsev, G. Rugel, A. Türler, Direct search for primordial ^{244}Pu. Geochim. Cosmochim. Acta Suppl. **73**, A713 (2009)

31. C. Wallner, T. Faestermann, U. Gerstmann, W. Hillebrandt, K. Knie, G. Korschinek, C. Lierse, C. Pomar, G. Rugel, Development of a very sensitive AMS method for the detection of supernova-produced longliving actinide nuclei in terrestrial archives. Nucl. Inst. Methods Phys. Res. B **172**(1–4), 333–337 (2000)
32. C. Wallner, T. Faestermann, U. Gerstmann, K. Knie, G. Korschinek, C. Lierse, G. Rugel, Supernova produced and anthropogenic ^{244}Pu in deep sea manganese encrustations. New Astron. Rev. **48**(1–4), 145–150 (2004)
33. M. Paul, A. Valenta, I. Ahmad, D. Berkovits, C. Bordeanu, S. Ghelberg, Y. Hashimoto, A. Hershkowitz, S. Jiang, T. Nakanishi, K. Sakamoto, Experimental limit to interstellar ^{244}Pu abundance. Astrophys. J. Lett. **558**(2), L133–L135 (2001)
34. A. Wallner, T. Faestermann, J. Feige, C. Feldstein, K. Knie, G. Korschinek, W. Kutschera, A. Ofan, M. Paul, F. Quinto et al., Abundance of live ^{244}Pu in deep-sea reservoirs on Earth points to rarity of actinide nucleosynthesis. Nat. Commun. **6**, 5956 (2015)
35. A. Wallner, M.B. Froehlich, M.A.C. Hotchkis, N. Kinoshita, M. Paul, M. Martschini, S. Pavetich, S.G. Tims, N. Kivel, D. Schumann et al., ^{60}Fe and ^{244}Pu deposited on Earth constrain the r-process yields of recent nearby supernovae. Science **372**(6543), 742–745 (2021)
36. K. Hotokezaka, T. Piran, M. Paul, Short-lived ^{244}Pu points to compact binary mergers as sites for heavy r-process nucleosynthesis. Nat. Phys. **11**(12), 1042 (2015)
37. N.R. Tanvir, A.J. Levan, A.S. Fruchter, J. Hjorth, R.A. Hounsell, K. Wiersema, R.L. Tunnicliffe, A 'kilonova' associated with the short-duration γ-ray burst GRB 130603B. Nature **500**(7464), 547–549 (2013)
38. B.P. Abbott, R. Abbott, T.D. Abbott, F. Acernese, K. Ackley, C. Adams, T. Adams, P. Addesso, R.X. Adhikari, V.B. Adya et al., GW170817: observation of gravitational waves from a binary neutron star inspiral. Phys. Rev. Lett. **119**, 161101 (2017)
39. D. Breitschwerdt, J. Feige, M.M. Schulreich, M.A. De, C. Avillez, B.F. Dettbarn, The locations of recent supernovae near the Sun from modelling ^{60}Fe transport. Nature **532**(7597), 73–76 (2016)
40. M. Kachelrieß, A. Neronov, D.V. Semikoz, Signatures of a two million year old supernova in the spectra of cosmic ray protons, antiprotons, and positrons. Phys. Rev. Lett. **115**(18), 181103 (2015)
41. G.J. Wasserburg, M. Busso, R. Gallino, K.M. Nollett, Short-lived nuclei in the early solar system: possible AGB sources. Nucl. Phys. A **777**, 5–69 (2006)
42. M. Lugaro, A.I. Karakas, ^{26}Al and ^{60}Fe yields from AGB stars. New Astron. Rev. **52**(7–10), 416–418 (2008)
43. M. Lugaro, A. Chieffi, Radioactivites in low- and intermediate-mass stars, in *Lecture Notes in Physics*, vol. 812, ed. by R. Diehl, D.H. Hartmann, N. Prantzos (Springer, Berlin, 2011), pp.83–152
44. R. Diehl, A.J. Korn, B. Leibundgut, M. Lugaro, A. Wallner, Cosmic nucleosynthesis: a multi-messenger challenge. Prog. Part. Nucl. Phys. **127**, 103983 (2022)
45. M. Honda, M. Imamura, Half-life of ^{53}Mn. Phys. Rev. C **4**, 1182–1188 (1971)
46. N. Altobelli, F. Postberg, K. Fiege, M. Trieloff, H. Kimura, V.J. Sterken, H.W. Hsu, J. Hillier, N. Khawaja, G. Moragas-Klostermeyer et al., Flux and composition of interstellar dust at Saturn from Cassini's Cosmic Dust Analyzer. Science **352**(6283), 312–318 (2016)
47. M. Landgraf, *Variations of the Interstellar Dust Distribution in the Heliosphere* (Springer Netherlands, Dordrecht, 2006), pp.195–208
48. M. Horányi, Z. Sternovsky, M. Lankton, C. Dumont, S. Gagnard, D. Gathright, E. Grün, D. Hansen, D. James, Kempf, The lunar dust experiment (LDEX) onboard the lunar atmosphere and dust environment explorer (LADEE) mission. Sp. Sci. Rev. **185**(1–4), 93–113 (2014)
49. B.J. Fry, B.D. Fields, J.R. Ellis, A. Shrapnel, Discriminating among near-Earth stellar explosion sources of live radioactive isotopes. Astrophys. J. **800**(1), 71 (2015)
50. G.J. Feldman, R.D. Cousins, Unified approach to the classical statistical analysis of small signals. Phys. Rev. D **57**, 3873–3889 (1998)
51. D.E. Gault, F. Hoerz, D.E. Brownlee, J.B. Hartung, Mixing of the lunar regolith. Lunar Planet. Sci. Conf. Proc. **3**, 2365–2386 (1974)
52. D. Koll, G. Korschinek, T. Faestermann, J.M. Gómez-Guzmán, S. Kipfstuhl, S. Merchel, J.M. Welch, Interstellar ^{60}Fe in Antarctica. Phys. Rev. Lett. **123**(7), 072701 (2019)
53. A. Wallner, J. Feige, L.K. Fifield, M.B. Froehlich, R. Golser, M.A.C. Hotchkis, D. Koll, G. Leckenby, M. Martschini, S. Merchel et al., ^{60}Fe deposition during the late Pleistocene and the Holocene echoes past supernova activity. Proc. Natl. Acad. Sci. **117**(36), 21873–21879 (2020)
54. A. Wallner, J. Feige, L.K. Fifield, M.B. Froehlich, R. Golser, M.A.C. Hotchkis, D. Koll, G. Leckenby, M. Martschini, S. Merchel et al., ^{60}Fe deposition during the late Pleistocene and the Holocene echoes past supernova activity. Proc. Natl. Acad. Sci. **117**(36), 21873–21879 (2020)
55. D. Koll, T. Faestermann, G. Korschinek, A. Wallner, Origin of recent interstellar ^{60}Fe on Earth. Eur. Phys. J. Web Conf. **232**, 02001 (2020)
56. P.C. Frisch, The nearby interstellar medium. Nature **293**(5831), 377–379 (1981)
57. D.P. Cox, R.J. Reynolds, The local interstellar medium. Annu. Rev. Astron. Astrophys. **25**, 303–344 (1987)
58. C. Zucker, A.A. Goodman, J. Alves, S. Bialy, M. Foley, J.S. Speagle, J. Großschedl, D.P. Finkbeiner, A. Burkert, D. Khimey, C. Swiggum, Star formation near the Sun is driven by expansion of the Local Bubble. Nature **601**(7893), 334–337 (2022)
59. P.C. Frisch, J.D. Slavin, Short-term variations in the galactic environment of the Sun. In: P.C. Frisch, editor, Solar Journey: The Significance of our Galactic Environment for the Heliosphere and Earth, volume 338 of Astrophysics and Space Science Library, p. 133 (2006)
60. N. Benítez, J. Maíz-Apellániz, M. Canelles, Evidence for nearby supernova explosions. Phys. Rev. Lett. **88**, 081101 (2002)
61. B.J. Fry, B.D. Fields, J.R. Ellis, Radioactive iron rain: transporting ^{60}Fe in supernova dust to the ocean floor. Astrophys. J. **827**(1), 48 (2016)
62. M.M. Schulreich, D. Breitschwerdt, J. Feige, C. Dettbarn, Numerical studies on the link between radioisotopic signatures on Earth and the formation of the Local Bubble. I. ^{60}Fe transport to the solar system by turbulent mixing of ejecta from nearby supernovae into a locally homogeneous interstellar medium. Astron. Astrophys. **604**, 81 (2017)
63. M. Schulreich, D. Breitschwerdt, J. Feige, C. Dettbarn, A Way Out of the Bubble Trouble?–Upon Reconstructing the Origin of the Local Bubble and Loop I via Radioisotopic Signatures on Earth. Galaxies **6**(1), 26 (2018)
64. R. Neuhäuser, F. Gießler, V.V. Hambaryan, A nearby recent supernova that ejected the runaway star ζ Oph, the pulsar PSR B1706–16, and ^{60}Fe found on Earth. Mon. Not. R. Astron. Soc. **498**(1), 899–917 (2020)
65. G. Briceño-Morales, J. Chanamé, Substructure, supernovae, and time resolved star formation history for Upper Scorpius (2022). arXiv e-prints arXiv:2205.01735
66. W.R. Binns, M.H. Israel, E.R. Christian, A.C. Cummings, G.A. de Nolfo, K.A. Lave, R.A. Leske, R.A. Mewaldt, E.C. Stone, T.T. von Rosenvinge, M.E. Wiedenbeck, Observation of the ^{60}Fe nucleosynthesis-clock isotope in galactic cosmic rays. Science **352**(6286), 677–680 (2016)
67. M.S. Basunia, Nuclear data sheets for A=59. Nucl. Data Sheets **151**, 1–333 (2018)

68. M.E. Wiedenbeck, W.R. Binns, E.R. Christian, A.C. Cummings, B.L. Dougherty, P.L. Hink, J. Klarmann, R.A. Leske, M. Lijowski, R.A. Mewaldt et al., Constraints on the time delay between nucleosynthesis and cosmic-ray acceleration from observations of ^{59}Ni and ^{59}Co. Astrophys. J. **523**(1), L61–L64 (1999)
69. M.J. Boschini, S. Della Torre, M. Gervasi, D. Grandi, G. Jóhannesson, G. La Vacca, N. Masi, I.V. Moskalenko, S. Pensotti, T.A. Porter et al., The discovery of a low-energy excess in cosmic-ray iron: evidence of the past supernova activity in the local bubble. Astrophys. J. **913**(1), 5 (2021)
70. M. Aguilar, L. Ali Cavasonza, M.S. Allen, B. Alpat, G. Ambrosi, L. Arruda, N. Attig, F. Barao, L. Barrin, Bartoloni, Properties of iron primary cosmic rays: results from the alpha magnetic spectrometer. Phys. Rev. Lett. **126**(4), 041104 (2021)
71. K.D. Terry, W.H. Tucker, Biologic effects of supernovae. Science **159**(3813), 421–423 (1968)
72. M.A. Ruderman, Possible consequences of nearby supernova explosions for atmospheric ozone and terrestrial life. Science **184**(4141), 1079–1081 (1974)
73. J. Ellis, D.N. Schramm, Could a nearby supernova explosion have caused a mass extinction? Proc. Natl. Acad. Sci. **92**, 235–238 (1995)
74. B.C. Thomas, E.E. Engler, M. Kachelrieß, A.L. Melott, A.C. Overholt, D.V. Semikoz, Terrestrial effects of nearby supernovae in the early pleistocene. Astrophys. J. Lett **826**(1), L3 (2016)
75. A.L. Melott, B.C. Thomas, M. Kachelrieß, D.V. Semikoz, A.C. Overholt, A supernova at 50 pc: effects on the Earth's atmosphere and biota. Astrophys. J. **840**(2), 105 (2017)
76. A.L. Melott, B.C. Thomas, Terrestrial effects of moderately nearby supernovae. Lethaia **51**(3), 325–329 (2018)
77. A.L. Melott, B.C. Thomas, From cosmic explosions to terrestrial fires? J. Geol. **127**(4), 475–481 (2019)
78. N. Marsh, H. Svensmark, Solar influence on Earth's climate. Sp. Sci. Rev. **107**, 317–325 (2003)
79. I.G. Usoskin, G.A. Kovaltsov, Cosmic rays and climate of the Earth: possible connection. C.R. Geosci. **340**(7), 441–450 (2008)
80. J. Kirkby, Cosmic rays and climate. Surv. Geophys. **28**(5–6), 333–375 (2007)
81. N. Shaviv, J. Veizer, Celestial driver of Phanerozoic climate. GSA Today **13**(7), 4–10 (2003)
82. M.J. Orgeira, V.M.V. Herrera, L. Cappellotto, R.H. Compagnucci, Statistical analysis of the connection between geomagnetic field reversal, a supernova, and climate change during the Plio-Pleistocene transition. Int. J. Earth Sci. **111**(4), 1357–1372 (2022)
83. M. Opher, A. Loeb, Terrestrial impact from the passage of the solar system through a cold cloud a few million years ago. arXiv e-prints (2022) arXiv:2202.01813
84. B.P. Demenocal, Plio-pleistocene African climate. Science **270**(5233), 53–59 (1995)
85. G. Korschinek, Mass extinctions and supernova explosions. In: A. W. Alsabti, P. Murdin, editors, Handbook of Supernovae, p. 2419 (2017)
86. T. Faestermann, Dust from "recent" supernovae, just around the corner. In: The Sixth Saudi International Meeting on Frontiers of Physics 2018 (SIMFP2018), Volume 1976 of American Institute of Physics Conference Series, p. 020001 (2018)
87. C.D. Bacon, D. Silvestro, C. Jaramillo, B. Tilston Smith, P. Chakrabarty, A. Antonelli, Biological evidence supports an early and complex emergence of the Isthmus of Panama. Proc. Natl. Acad. Sci. **112**(19), 6110–6115 (2015)
88. N. Owen-Smith, Ecological links between African Savanna environments, climate change, and early hominid evolution, in *African Biogeography, Climate Change and Human Evolution, Chapter 10*. ed. by T.G. Bromage, F. Schrenk (Oxford University Press, Oxford, 1999), pp.138–149
89. B.P. Demenocal, Climate and human evolution. Science **331**(6017), 540–542 (2011)
90. F. Schrenk, T.G. Bromage, C.G. Betzler, U. Ring, Y.M. Juwayeyi, Oldest Homo and Pliocene biogeography of the Malawi Rift. Nature **365**(6449), 833–836 (1993)
91. A. Timmermann, K.-S. Yun, P. Raia, J. Ruan, A. Mondanaro, E. Zeller, C. Zollikofer, M. Ponce de León, D. Lemmon, M. Willeit, A. Ganopolski, Climate effects on archaic human habitats and species successions. Nature **604**(7906), 495–501 (2022)